



Contents lists available at SciVerse ScienceDirect

Surface & Coatings Technology

journal homepage: www.elsevier.com/locate/surfcoat

Exchange bias effects of NiFe/NiO bilayers through ion-beam bombardment on the NiO surface

Guijun Li ^a, Chi Wah Leung ^b, Chin Shueh ^c, Hsun-Feng Hsu ^c, Hsuan-Rong Huang ^c, Ko-Wei Lin ^{c,*}, Pui To Lai ^a, Philip W.T. Pong ^{a,*}

^a Department of Electrical and Electronic Engineering, The University of Hong Kong, Hong Kong, Hong Kong

^b Department of Applied Physics, Hong Kong Polytechnic University, Hong Kong, Hong Kong

^c Department of Materials Science and Engineering, National Chung Hsing University, Taichung, Taiwan

ARTICLE INFO

Available online xxxx

Keywords:

Exchange bias
Ion-beam bombardment
Magnetic thin films

ABSTRACT

The influence of ion-beam bombardment of the NiO surface on the exchange bias behavior of NiFe/NiO bilayers was systematically investigated with different bombardment energies and durations. The results show that by varying the bombardment energies, different crystallographic orientations are created which modifies the NiO spin structures. This results in the changes in the coupling type in NiO when it is in contact with the NiFe layer. The NiFe/NiO bilayers exhibited either enhanced or decreased exchange bias field, depending on the uncompensated moments or misaligned NiO spin created by ion-beam bombardment. The variations in coercivities of NiFe/NiO bilayers imply that the NiO anisotropy could be tuned by ion-beam bombardment.

© 2012 Elsevier B.V. All rights reserved.

1. Introduction

Exchange bias is a phenomenon, which provides the pinning field for ferromagnetic layer [1–3] and also increases the ferromagnetic layer coercivity [4–7]. A ferromagnetic (FM)/antiferromagnetic (AF) bilayer structure is the most common configuration. After cooling through the Neel temperature of AF layer, the exchange bias effect can be set into the system [8–10]. With a field-cooling process, the final exchange bias field can be either positive or negative, and it can be tuned by bombardment of moderate-energy Ar ions on the AF layer surface [11–13].

Ion beam bombardment during the thin film growth process can influence the film properties including adhesion, nucleation, internal stress, morphology, and composition [14–16]. Pranevicius previously studied the influence of ion-beam bombardment on the nucleation of thin film during deposition [14]. It was found that with no bombardment process during the Al film growth at a rate of 10^{16} atoms/cm²-s, a considerable incubation time (40 s) was required before the superimposed growth of Al islands. On the other hand, the presence of ion-beam bombardment (5 keV Ar) would decrease the overlap time duration to 15 s, due to the increased nucleation sites produced for island formation and growth. The grain size of thin films shows complicated dependence on the ion beam energy [15]. Most metals show significant decreases in grain sizes with increasing ion beam

energy. It was argued that the ions becomes incorporated at the grain boundaries during the film growth process, and an ion beam of sufficiently high energy may inhibit the grain growth; also high beam energies can lead to irradiation-induced lattice disorders that would limit the grain growth [15]. The influence of ion-beam bombardment on the surface roughness was modeled using molecular dynamics simulations, and it was found that the thin film deposition with ion-beam bombardment could remove coated atoms via sputtering [16].

NiO as an AF material has been widely investigated as the pinning layer in magnetoresistive spin valve structures [17–20]. Sputtered NiFe/NiO bilayers possess a blocking temperature as high as 230 °C and an exchange bias field of 20 Oe [21]. The NiO film morphology would influence the properties of the ferromagnetic underlayer. Smaller grain sizes of NiO layer with diameter of 12 nm exhibited an exchange bias field of 20 Oe, which is two-times larger than that of similar structure but with larger grains of 37 nm [22]. Larger surface roughness of NiO layer is found to introduce larger coercivity (10 Oe) than smooth NiFe/NiO bilayer (5 Oe) [23]. In addition, Yu et al. [24] reported that the formation of magnetic defects due to interface reaction strongly affects both coercivities as well as exchange bias field. Also, Lee et al. [25] reported that nonmagnetic second phase (Ni₂O₃) formed during fabrication of the NiO layer may destroy the NiO antiferromagnetism and thus weaken the exchange coupling in a NiFe/NiO bilayer.

We previously investigated a series of different exchange bias bilayers. For example, the exchange bias fields of NiFe/NiO bilayers are strongly influenced by the ratio of oxygen and Ar, due to the expanded NiO structures formed during fabrication processes [26].

* Corresponding authors.

E-mail addresses: kwlin@dragon.nchu.edu.tw (K-W. Lin), ppong@eee.hku.hk (P.W.T. Pong).

Using different oxygen/argon flow rate ratios ranging from 8% to 26% during the Cr-oxide sputtering process, the exchange bias field of NiFe/Cr-oxide bilayer changed from -25 to -75 Oe [27]. Using different ion bombardment voltages from 70 to 150 V during sputtering, the exchange bias field of NiFe/Mn bilayer changed from -250 to -400 Oe [28]. Thus we found that the exchange bias could be modified by energetic Ar ion-beam bombardment. However, a widely studied exchange bias system of NiFe/NiO bilayer has not been investigated by ion-beam bombardment so far.

In this study, we investigated the exchange bias behavior in NiFe/NiO bilayers with different ion-beam bombardment voltages (from 0 to 150 V) and different bombardment durations (from 1 min to 20 min) on the surface of the bottom NiO layer. It was found that by using higher ion-beam bombardment energy or longer bombardment duration, the changes in NiO crystallographic orientations may affect the corresponding spin structures and give rise to the polarity switch in exchange bias fields.

2. Experiments

A dual ion-beam deposition technique [29] was used to sputter NiFe (8 nm)/NiO (15 nm) bilayers on the SiO₂ substrates. A Kaufman ion source was used to bombard the Ni target with 3 sccm Ar and the End-Hall ion source was used to bombard the SiO₂ substrate with 2.6 sccm Ar and 0.5 sccm O₂ to oxidize Ni into NiO in-situ [30]. Then the NiO surface was either bombarded with different ion-beam bombardment energies (V_{EH}) from 0 to 150 V for 5 min, or bombarded for different durations (1–20 min) with $V_{EH} = 150$ V to induce changes on the NiO surface conditions. After that the Kaufman ion source was used to focus the argon ion-beam onto a commercial Ni₈₀Fe₂₀ (at%) target surface for depositing the NiFe layer on top of the NiO layer. The crystalline structures of the NiFe/NiO bilayers were characterized by a Bruker x-ray diffractometer (XRD). Magnetic measurements were performed in a commercial SQUID magnetometer (Quantum Design MPMS), where the thin films were field-cooled (FC) with a 20 kOe in-plane magnetic field from 300 K down to 5 K. The surface morphology of the bottom NiO layer was characterized by a NT-MDT Solver Pro-M atomic force microscope (AFM).

3. Results and discussion

To characterize the crystalline structure and composition of the sputtered NiFe (8 nm)/NiO (15 nm) bilayers, the samples bombarded with different ion-beam energies and durations were investigated with XRD. The XRD spectra of NiFe/NiO bilayers with different ion-beam bombardment energies ($V_{EH} = 0$ –150 V) are shown in Fig. 1. The structures of the NiFe/NiO bilayers were determined to be fcc NiFe (lattice constant $a \sim 3.55$ Å) and rock-salt NiO ($a \sim 4.21$ Å), as revealed by the diffraction peaks of (111) and (200) of NiFe and (111), (200), (220) of NiO, respectively. This is consistent with those reported in our previous work [30]. However, as the ion-beam bombardment energy was increased from 0 to 150 V, the peak ratio of (111)/(200) in NiO was found to decrease with increasing ion-beam bombardment energies, as shown in the inset of Fig. 1. The reason for the change in the peak ratio is likely attributed to the changes in preferred orientations due to ion-beam bombardment, as observed in our previous work [31]. This in turn changes the spin/magnetic structures and affects the corresponding exchange bias effects when the NiO layer is capped with a top NiFe layer. In addition, the peak positions in XRD spectra in Fig. 1 did not change indicating no new phases were formed after the ion-beam bombardment. Instead, the role of varying the ion-beam bombardment energies seems to change the preferred orientations of NiO layers. This in turn changes the magnetic anisotropy in NiO and affects the corresponding magnetic properties in NiFe/NiO bilayers.

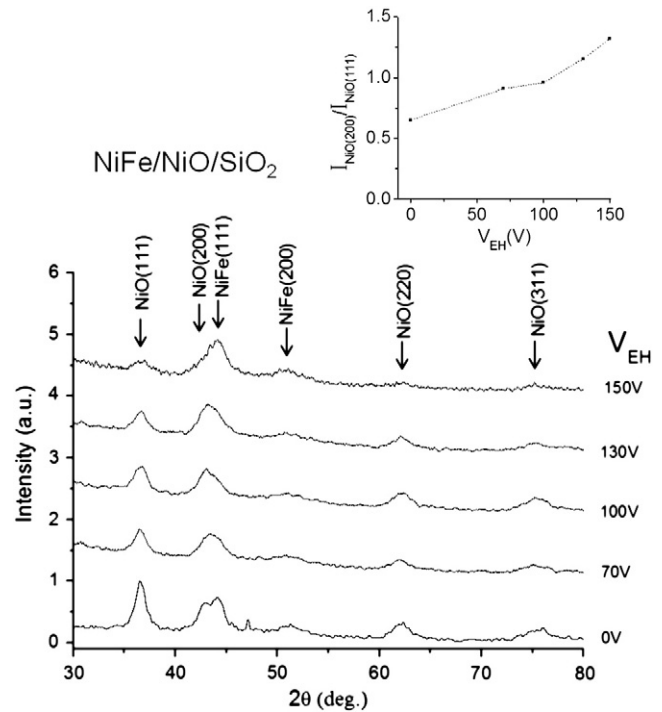


Fig. 1. X-ray diffraction spectra of the NiFe/NiO bilayers with different ion-beam bombardment energies ($V_{EH} = 0$ –150 V).

To further probe the ion-beam bombardment effects on the antiferromagnetic NiO layers in NiFe/NiO bilayers, the ion-beam bombardment energy was fixed at $V_{EH} = 150$ V and the NiO layers were bombarded with different durations (1–20 min). The results are shown in Fig. 2. It is seen that at low ion-beam bombardment durations (1, 2, and 5 min), two peaks of NiO (200) and NiFe (111) are still resolved. In contrast, increasing the ion-beam bombardment durations (10 and 20 min) resulted in the peak broadening ($2\theta \sim 42^\circ$) of NiO (200) that is attributed to the grain size refinement due to ion-beam bombardment. In addition, no diffraction peak shift in NiO was observed at all ion-beam bombardment durations. This indicates that varying the ion-beam bombardment durations (and thus irradiation dosages) changes the NiO grain sizes while the rock-salt NiO structures remain unchanged, as evidenced by the same NiO lattice constants ($a \sim 4.21$ Å). The above

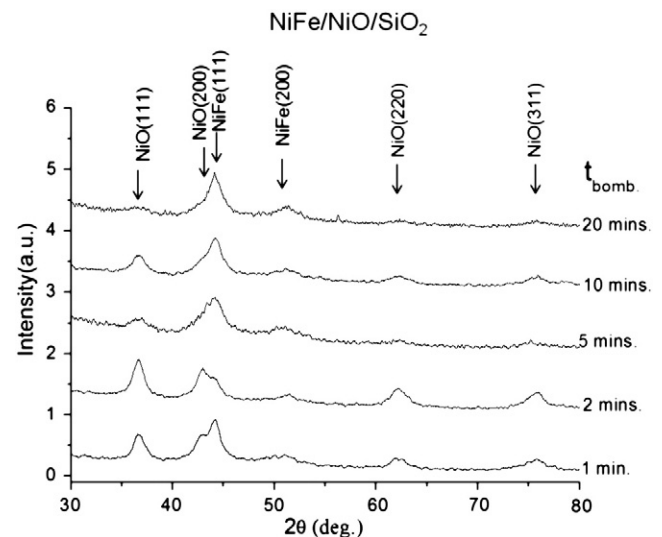


Fig. 2. X-ray diffraction spectra of the NiFe/NiO bilayers with different ion-beam bombardment durations ($t_{bomb} = 1$ –20 min).

results led us to conclude that the roles of ion-beam bombardment are two-folds: changing the crystallographic orientations (different energy regimes, with results shown in Fig. 1) and grain size refinements (different irradiation dosages, with results shown in Fig. 2).

In order to investigate the changes in NiO surface morphology due to ion-beam bombardment, AFM was used to characterize the surface morphology and the results are shown in Fig. 3. Our previous work [30] shows that increasing the ion-beam bombardment energy ($V_{EH} = 0$ V to 150 V) results in the reduction of the NiO surface roughness (from ~ 0.6 nm ($V_{EH} = 0$ V) to ~ 0.4 nm ($V_{EH} = 150$ V)). In addition, the changes in surface morphology (irregular or stripe-like texture) were observed. Further, a different evolution in surface morphology was observed after bombarding the NiO surface with different durations. Upon bombarding for 1 min ($t_{bomb.} = 1$ min), the surface roughness increased to ~ 1.6 nm with isolated grains, as shown in Fig. 3(a). As the ion-beam bombardment duration was increased to 2 min, the surface roughness decreased to ~ 0.8 nm (Fig. 3 (b)), indicating a smoother surface formed. As the bombardment duration further increased to 20 min, the sample surface roughness decreased to ~ 0.7 nm, as shown in Fig. 3(c). The above results suggest that longer bombardment duration would result in a smoother surface. Therefore, we conclude that the ion-beam bombardment changes the surface morphology and the flattened surface can be acquired using higher bombardment energy or longer bombardment duration.

The magnetic properties of NiFe/NiO bilayers bombarded with different ion-beam energies and durations were characterized by SQUID magnetometry. The hysteresis loops as well as coercivities (H_c) and exchange bias fields (H_{ex}) of the NiFe/NiO bilayers measured as a function of the ion-beam bombardment energy at 5 K under a 20 kOe field-cooling process are given in Fig. 4. The exchange bias field of the NiFe/NiO bilayer first decreased as the End–Hall voltage increased till $V_{EH} = 100$ V, then a larger exchange bias of $H_{ex} \sim -135$ Oe was obtained with $V_{EH} = 130$ V (Fig. 4(a)). When the End–Hall energy was $V_{EH} = 150$ V, a positive exchange bias field of $H_{ex} \sim 190$ Oe was obtained with the asymmetric hysteresis loop shown in Fig. 4(b). On the other hand, the coercivity changed slightly as the End–Hall voltage increased, and the highest coercivity of $H_c \sim 235$ Oe was obtained with $V_{EH} = 100$ V. The coercivity then decreased as the End–Hall voltage further increased till $V_{EH} = 150$ V, as shown in Fig. 4(c).

The unusual exchange bias behavior can be explained based on the type of the interfacial coupling between FM and AF layers. Koon [32] showed by micromagnetic calculations that a perpendicular orientation exists between the FM/AF axis directions. The AF spins cant away from the FM direction if the microscopic exchange interaction between FM and AF spins (J_{FM-AF}) is antiferromagnetic whereas they cant toward the FM direction if J_{FM-AF} is ferromagnetic. This has been successfully applied to explain the origin of the positive exchange bias in Fe/FeF₂ bilayers [33]. Further, Ijiri et al. [34] demonstrated the link between the exchange bias effect and the perpendicular coupling of the ferromagnetic and AF spins in epitaxial Fe₃O₄/CoO multilayers. The AF spins were found to align perpendicularly to an applied field. This results from frustration due to interfacial exchange coupling to the FM spins. In our NiFe/NiO bilayers, when the End–Hall voltage was below $V_{EH} = 130$ V, the bottom antiferromagnetic NiO layer exhibited ferromagnetic coupling (FM coupling) with the adjacent NiFe layer, which leads to the usual negative exchange bias [35]. The only observed positive exchange bias field in NiFe/NiO ($V_{EH} = 150$ V) bilayer is likely attributed to the changes in crystallographic orientations (as evidenced by the XRD in Fig. 1) and thus resulted in canted NiO spin structures. This canted NiO spin structures may couple antiferromagnetically (AF coupling) to the NiFe layer and thus give rise to the observed positive H_{ex} . This is in agreement with the results reported in our previous work in NiFe/(Ni,Fe)O bilayers [35].

The exchange bias behavior of NiFe/NiO bilayers with different ion-beam bombardment durations on the NiO surface is shown in Fig. 5. The NiFe/NiO ($t_{bomb.} = 2$ min) bilayers exhibited a symmetric hysteresis loop (Fig. 5(a)) with a small negative exchange bias field ($H_{ex} \sim -25$ Oe). However, increasing the ion-beam bombardment duration to 5 min, the exchange bias field of NiFe/NiO bilayers changed its polarity from negative to positive ($H_{ex} \sim +195$ Oe). The magnitude of the positive H_{ex} decreased with increasing ion-beam bombardment durations, accompanied by the asymmetry in hysteresis loop, as shown in Fig. 5(b). The largest positive H_{ex} may result from the uncompensated moments created [28] in moderate ion-beam bombardment durations. The change in H_{ex} polarity is similar to that observed in Fig. 4 (i.e., mechanism related to the FM or AF coupling), whereas the drop in positive H_{ex} (vs. $t_{bomb.}$, shown in Fig. 5(c)) is attributed to the increased degree of the spin misalignment [36] created on the NiO surface due to longer ion-

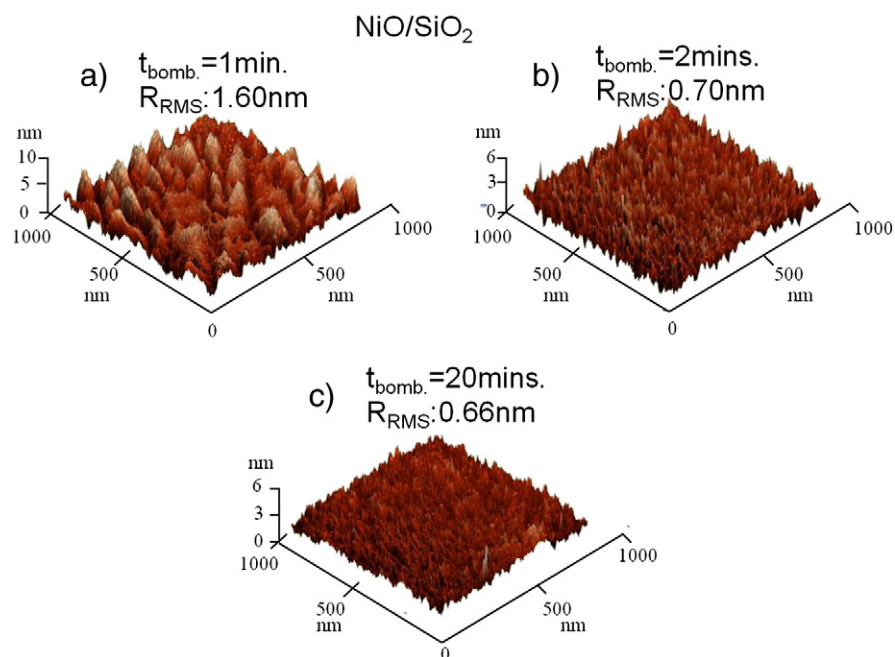


Fig. 3. AFM images of ion-beam bombarded ($V_{EH} = 150$ V) NiO surfaces with different bombardment durations: (a) 1 min, (b) 2 min, and (c) 20 min, respectively.

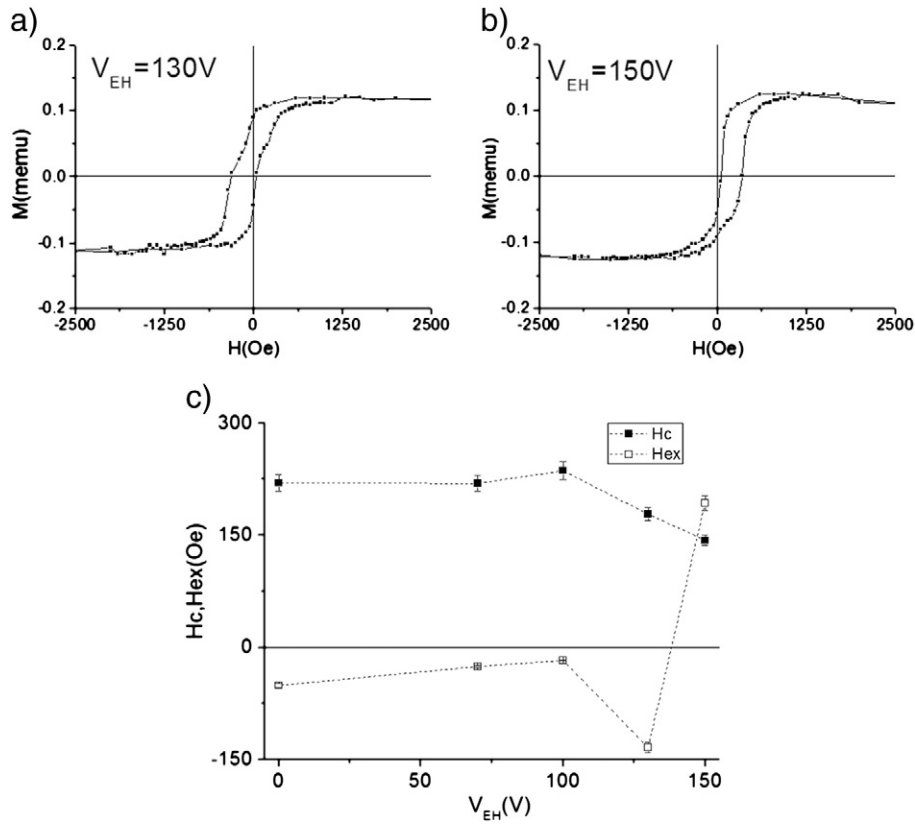


Fig. 4. The hysteresis loops of NiFe/NiO bilayers (5 K under a 20 kOe field-cooling process) with different ion-beam bombardment energies: (a) $V_{EH} = 130$ V and (b) $V_{EH} = 150$ V. The dependence of H_{ex} and H_c on V_{EH} in NiFe/NiO bilayers is shown in (c).

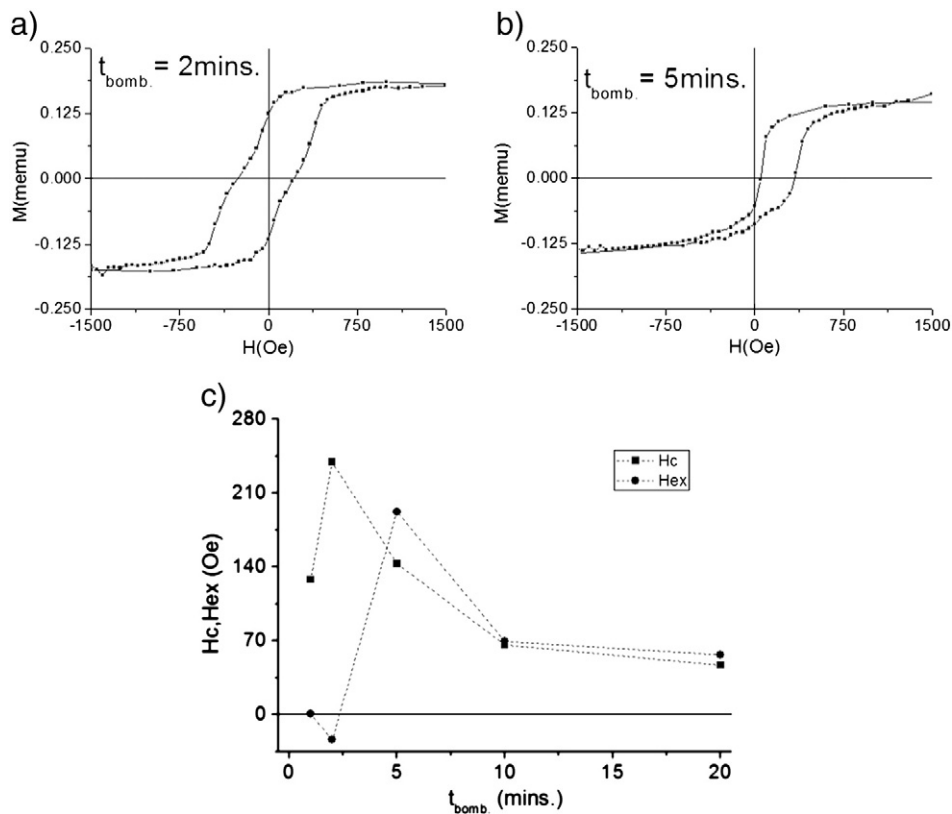


Fig. 5. The hysteresis loops of NiFe/NiO bilayers (5 K under a 20 kOe field-cooling process) with different ion-beam bombardment durations: (a) $t_{bomb} = 2$ min and (b) $t_{bomb} = 5$ min. The dependence of H_{ex} and H_c on t_{bomb} in NiFe/NiO bilayers is shown in (c).

beam bombardment durations. On the other hand, as the bombardment duration increased, the corresponding coercivity first increased to a maximum of $H_c \sim 240$ Oe with $t_{\text{bomb.}} = 2$ min, then decreased as the bombardment duration further decreased. This implies that the NiO anisotropy (K) could be modified [37,38] (enhanced or reduced K depending on the bombardment durations) and affects the exchange bias properties when it is in contact with the top NiFe layer.

4. Conclusion

The exchange bias effects of NiFe/NiO bilayers were studied by bombarding the bottom NiO surface with different ion-beam energies (V_{EH}) and durations ($t_{\text{bomb.}}$). It was shown that the coupling type (FM or AF coupling between NiFe and NiO layers) may give rise to the observed negative or positive exchange bias field through ion-beam bombardment which changes the NiO crystallographic orientations (thus spin structures). The enhanced or drop in coercivities of NiFe/NiO bilayers is attributed to the changes in NiO anisotropies with different ion-beam bombardment durations on the NiO surfaces. These results indicate that the exchange bias properties of NiFe/NiO bilayers could be modulated through the ion-beam bombardment.

Acknowledgement

This work was supported by the Seed Funding Program for Basic Research from the University of Hong Kong, the RGC-GRF grant (HKU 7049/11P), the RGC-GRF grant (PolyU 5013/08P) and the National Science Council of Taiwan.

References

- [1] M. Doi, M. Izumi, H. Endo, H.N. Fuke, H. Iwasaki, M. Sahashi, *IEEE Trans. Magn.* 41 (2005) 2932.
- [2] C. Binek, S. Polisetty, X. He, A. Berger, *Phys. Rev. Lett.* 96 (2006) 067201.
- [3] A. Tanaka, Y. Shimizu, H. Kishi, K. Nagasaka, H. Kanai, M. Oshiki, *IEEE Trans. Magn.* 35 (1999) 700.
- [4] S.Y. Yin, S.L. Yuan, Z.M. Tian, L. Liu, C.H. Wang, X.F. Zheng, H.N. Duan, S.X. Huo, *J. Appl. Phys.* 107 (2010) 043909.
- [5] M. Reinhardt, J. Seifert, M. Busch, H. Winter, *Phys. Rev. B* 81 (2010) 134433.
- [6] C. Fleischmann, F. Almeida, J. Demeter, K. Paredis, A. Teichert, R. Steitz, S. Brems, B. Opperdoes, C. van Haesendonck, A. Vantomme, K. Temst, *J. Appl. Phys.* 107 (2010) 113907.
- [7] N.N. Shams, M.T. Rahman, C.H. Lai, *J. Appl. Phys.* 105 (2009) 07D722.
- [8] S. Anandakumar, V.S. Rani, S. Oh, C. Kim, *Thin Solid Films* 519 (2010) 1020.
- [9] R. Morales, Z.P. Li, J. Olamit, K. Liu, J.M. Alameda, I.K. Schuller, *Phys. Rev. Lett.* 102 (2009) 097201.
- [10] X. He, Y. Wang, N. Wu, A.N. Caruso, E. Vescovo, K.D. Belashchenko, P.A. Dowben, C. Binek, *Nat. Mater.* 9 (2010) 579.
- [11] D. Schafer, P.L. Grande, L.G. Pereira, J. Geshev, *J. Appl. Phys.* 109 (2011) 023905.
- [12] A. Ehresmann, C. Schmidt, T. Weis, D. Engel, *J. Appl. Phys.* 109 (2011) 023910.
- [13] C.H. Su, S.C. Lo, K.-W. Lin, J. van Lierop, H. Ouyang, *J. Appl. Phys.* 105 (2009) 033904.
- [14] L. Pranevicius, *Thin Solid Films* 63 (1979) 77.
- [15] C. Spinella, S. Lombardo, F. Priolo, *J. Appl. Phys.* 84 (1998) 5383.
- [16] A. Robbmond, B.J. Thijsse, *Nucl. Instrum. Methods B* 127 (1997) 273.
- [17] C. Cowache, B. Dieny, S. Auffret, M. Cartier, R.H. Taylor, R. O'Barr, S.Y. Yamamoto, *IEEE Trans. Magn.* 34 (1998) 843.
- [18] S.S. Lee, D.G. Hwang, C.M. Park, K.A. Lee, *IEEE Trans. Magn.* 33 (1997) 3547.
- [19] S.X. Li, T.S. Plaskett, P.P. Freitas, J. Bernardo, B. Almeida, J.B. Sousa, *IEEE Trans. Magn.* 34 (1998) 3772.
- [20] T. Lin, D. Mauri, *IEEE Trans. Magn.* 35 (1999) 2607.
- [21] S. Soeya, T. Imagawa, K. Mitsuoka, S. Narishige, *J. Appl. Phys.* 76 (1994) 5356.
- [22] C.H. Nam, B.K. Cho, S. Lee, *J. Appl. Phys.* 93 (2003) 6584.
- [23] D.G. Hwang, S.S. Lee, C.M. Park, *J. Magn. Magn. Mater.* 199 (1999) 39.
- [24] G.H. Yu, C.L. Chai, F.W. Zhu, J.M. Xiao, W.Y. Lai, *J. Appl. Phys.* 78 (2001) 1706.
- [25] D.H. Lee, S.Y. Yoon, D.H. Yoon, S.J. Suh, *J. Korean Phys. Soc.* 44 (2004) 1079.
- [26] J.-Y. Guo, J. van Lierop, S.-Y. Chang, K.-W. Lin, *Jpn. J. Appl. Phys.* 48 (2009) 073004.
- [27] K.-W. Lin, J.-Y. Guo, *J. Appl. Phys.* 104 (2008) 123913.
- [28] K.-W. Lin, T.-J. Chen, J.-Y. Guo, H. Ouyang, D.-H. Wei, J. van Lierop, *J. Appl. Phys.* 105 (2009) 07D710.
- [29] R. Magaraggia, M. Kostylev, R.L. Stamps, K.-W. Lin, J.-Y. Guo, K.-J. Yang, R.D. Desautels, J. van Lierop, *IEEE Trans. Magn.* 47 (2011) 1614.
- [30] K.-W. Lin, M. Mirza, C. Shueh, H.-R. Huang, H.-F. Hsu, J. van Lierop, *J. Appl. Phys.* 100 (2012) 122409.
- [31] K.-W. Lin, M.-R. Wei, J.-Y. Guo, *J. Nanosci. Nanotechnol.* 9 (2009) 2023.
- [32] N.C. Koon, *Phys. Rev. Lett.* 78 (1997) 4865.
- [33] J. Nogues, D. Lederman, T. Moran, I.K. Schuller, *Phys. Rev. Lett.* 76 (1996) 3186.
- [34] Y. Ijiri, T.C. Schulthess, J.A. Borchers, P.J. van der Zaag, R.W. Erwin, *Phys. Rev. Lett.* 99 (2007) 147201.
- [35] K.-W. Lin, M.-R. Wei, J.-Y. Guo, *J. Nanosci. Nanotechnol.* 8 (2008) 1.
- [36] J. McCord, C. Hamann, R. Schafer, L. Schultz, R. Mattheis, *Phys. Rev. B* 78 (2008) 094419.
- [37] K.-W. Lin, J.-Y. Guo, T.-J. Chen, H. Ouyang, E. Vass, J. van Lierop, *J. Appl. Phys.* 104 (2008) 123908.
- [38] K.-W. Lin, V.V. Volobuev, J.-Y. Guo, S.-H. Chung, H. Ouyang, J. van Lierop, *J. Appl. Phys.* 107 (2010) 09D712.